ISSN 0006-3509, Biophysics, 2020, Vol. 65, No. 1, pp. 28–38. © Pleiades Publishing, Inc., 2020.
Russian Text © The Author(s), 2020, published in Biofizika, 2020, Vol. 65, No. 1, pp. 36–47.

MOLECULAR BIOPHYSICS

The Manifestation of Hysteresis in the Thermal Properties of Nanosystems Based on the Example of Supercooled Water Clusters in Wet Sephadex of the G Type

N. A. Grunina[a], *, T. V. Belopolskaya[b], G. I. Tsereteli[b], and O. I. Smirnova[b]

[a] *St. Petersburg State University of Civil Aviation, St. Petersburg, 196210 Russia*
[b] *St. Petersburg State University, St. Petersburg, Staryi Peterhof, 198504 Russia*
**e-mail: nagrunina@mail.ru*

Received June 7, 2019; revised November 26, 2019; accepted November 27, 2019

Abstract—The research cycle of thermal properties of water clusters in polysaccharide–water systems (starch and Sephadex G-100) with a low content of freezing water was continued based on the example of another modified polysaccharide, Sephadex G-25. This Sephadex has a more rigid three-dimensional structure compared with Sephadex G-100. The doublet structure of the melting curve of water clusters, which indicated the bimodal nature of their size distribution, was the main peculiarity of the data obtained for Sephadex G-25 by differential scanning calorimetry. The observed decrease in the temperature and heat of melting and crystallization of water clusters with a decrease in the humidity of Sephadex G-25, as in the case of other polysaccharides, was a typical manifestation of the size effect for nanosystems. At the same time, hysteresis occurred between the temperatures $\Delta T = T_{mel} - T_{cr}$, and the heats $\Delta Q = Q_{mel} - Q_{cr}$ of these transitions, which is also typical for small systems. It was found that the transformation processes (recrystallization, reorganization, and size change) in the system of clusters of crystallized supercooled water in Sephadex G-25 with low humidity during heating could occur both below the melting interval and inside it, which indicated the nonequilibrium state of the original set of nanoclusters. It was shown that the decrease of V_{heat}, as well as annealing within the melting interval led to a redistribution of clusters in size and, according to the revealed size effect, to an increase in the melting heat. These facts taken together indicated that the nonequilibrium state of the initially formed clusters during cooling and, as a consequence, their ability to transform with increasing temperature certainly play an important, if not a decisive, role in the manifestation of hysteresis in the thermal properties of water nanoclusters.

Keywords: calorimetry, water nanoclusters, Sephadex, crystallization, melting, transformation, size effect, hysteresis

DOI: 10.1134/S0006350920010078

INTRODUCTION

The study of various physical and chemical properties of small clusters (nanoparticles) is currently one of the priority areas of natural sciences (see, for example, the review [1] and numerous references in it). A significant increase in the surface-to-volume ratio in the case of nanoparticles in comparison with macroobjects gives them an entire complex of specific properties that differ from the properties of bulk matter. Great practical interest, in addition to the purely scientific interest in the study of nanoparticles, is due to the wide successful use of their unique properties in the technology of manufacturing a variety of high speed electronic devices, as well as in the creation of fundamentally new materials.

The first studies of the influence of size effects on the thermal properties of nanoparticles were conducted at the beginning of the last century [2]. In the 1970s–1980s, much attention was paid to the dependence of the melting temperature of nonequilibrium lamellar nanocrystals of synthetic polymers from their size [3–8]. In recent decades, studies of the relationship between the melting temperature and, more rarely, the melting heat with the size of clusters are only an insignificant part of the total number of the studies focused mainly on the electronic and optical properties of metal nanoparticles and simple compounds (see, for example, [9–13]). The thermal properties of nanoparticles are actively studied by computer modeling methods [14–19]. In addition, much attention is paid to experimental studies of nanoparticles embedded in solid-state matrices [20–23] or formed on a specially selected solid substrate [24–26]. A special place is occupied by the studies that consider clus-

Abbreviations: DSC, differential scanning calorimetry.

ters (nanoparticles) included in flexible mobile matrices [27–36] rather than in solid-state ones. However, the number of such studies is small.

The proposed study is among of the latter group. Biopolymers (various polysaccharides) are considered here as a flexible matrix at temperatures above their glass transition temperatures and water clusters embedded in them are the small particles. This work continues the cycle of our earlier studies by differential scanning calorimetry (DSC) of the thermal properties of supercooled water dispersed in wet natural and modified polysaccharides [36–39].

It has been reliably established that in biopolymers of various classes (proteins, DNA, and polysaccharides) that contain only a low percentage of freezing water, the thermal properties of water clusters demonstrate a size effect [27–39]. The temperature and heat of melting of water clusters in biopolymers depend on their size, namely, they significantly decrease with the decrease of size, as in the case of metal clusters or nanoparticles in solid-state matrices (see, for example, [25, 26, 40, 41]).

Moreover, in the study of the thermal properties of water clusters of two polysaccharide-water systems (starches and Sephadex G-100) by the sequential recording of the processes of melting and crystallization of the freezing water in the same sample by DSC we found a difference both between the temperatures and the heats of these transitions [36–39], that is, the existence of hysteresis between these two processes, as in other nanosystems [42–45]. We note that although this effect has been repeatedly observed for low-dimensional metal particles and simple compounds, there are still no generally accepted ideas about the causes of hysteresis in the thermal properties of nanoclusters; only some hypotheses are found in the literature. The difference between the thermal parameters of crystallization and melting of nanoparticles, which is absent in the macroscopic substance, has been predicted by theoretical studies [14, 15]. It is assumed that the main cause of the hysteresis is the coexistence of liquid and solid phases in the temperature region of the transition [42–44]. In a number of studies, the existing size distribution of clusters has been proposed as the cause of the observed hysteresis. This reason for the occurrence of hysteresis, as experimentally observed in the dependencies of various properties of metal and organic nanoclusters on the temperature during melting and solidification, was proposed in [45, 46].

The information presented above refers to nanoparticles that consist of low-molecular weight substances immersed in a medium that differs from them in chemical composition. Another situation occurs when small clusters are included in matrices of the same chemical composition. This applies to numerous studies of the thermal properties of partially crystalline synthetic polymers, in which the crystallites are immersed in an amorphous medium of the same polymer. It was found that reorganization of the initial crystallites of the nanometric scale occurs in the interval of their melting [3–8]. The fact that the crystallites are located in a medium that is absolutely identical to them in chemical composition made it possible to use the well-known Gibbs–Thomson formula to estimate their size [35]. In the most pronounced cases, the reorganization is manifested in the form of clearly expressed doublet melting curves; the ratio of the components of such a doublet depends on the heating conditions [3–8]. At the same time, in all the discussed studies, the reorganization is considered as a consequence of the nonequilibrium state of the initial crystallites formed during significant supercooling relative to the melting temperature.

The wet polysaccharides used in our study can be considered as intermediate between these two types of matrices. In polysaccharide-water systems, water clusters are located in a polymer matrix whose pore walls are covered with unfrozen water, that is, water clusters are immersed in a wet environment.

It has been shown in our studies in which hysteresis between the processes of melting and crystallization of water nanoclusters in polysaccharides was experimentally detected that the processes of transformation (reorganization) of the initial clusters formed during cooling can also occur in crystallized supercooled water during heating in the temperature region preceding the melting [37–39]. The hypothesis about possible transformation of starches was proposed on the basis of analysis and comparison of absolute values of the biopolymer heat capacity in the native and amorphous states [37, 38]. It was shown later in the study of the thermal properties of the modified polysaccharide Sephadex G-100 that the observed on the thermograms of heating the heat generation due to the additional crystallization of water clusters in the form of a clearly defined minimum in the region before the beginning of the melting interval was also a direct manifestation of their transformation [39].

In this study, the investigation of the processes of crystallization of supercooled water nanoclusters and their subsequent melting under variations of thermal modes of DSC measurements and sample humidity was continued with Sephadex G-25, as another example, which had a different and more rigid spatial structure of polysaccharide chains in comparison with G-100. At the same time, we hoped to obtain additional information about the transformation processes during heating of initially crystallized water clusters during cooling and, after combining it with the previously obtained information, to offer a possible explanation of the causes of hysteresis between the thermal parameters of their melting and crystallization. In our opinion, one of the causes of hysteresis may be the nonequilibrium state of water nanoclusters formed in polysaccharide-water systems with a low content of

freezing water, as in the case of polymer nanocrystallites.

MATERIALS AND METHODS

The measurements were made using a DSC-111 differential scanning calorimeter (SETARAM Instrumentation, France), whose sensitivity was 3×10^{-5} J/s. To study the processes of crystallization and melting of water clusters in Sephadexes with defined humidity, multiple cyclic measurements were performed in the cooling/heating mode in the temperature range from 25 to –60°C. The temperature scale of the calorimeter in both scanning modes was calibrated by the temperatures of reference substances, namely, indium, water, and mercury. The rate of heating and cooling of the samples in most experiments was the same and was equal to 5 deg/min. In some experiments, $V_{heat} = 1$ and 2 deg/min were used. The introduction of temperature corrections, depending on the V_{heat} and mass of the sample, in the temperature range outside the phase transitions was carried out in accordance with the data processing procedure developed by the manufacturer. The procedure for introducing corrections to the temperature values at the maxima of phase transitions obtained experimentally in the heating mode was described in detail previously [36, 37]. After taking the corrections into account, the error in the determination of the temperature of the studied transitions was ±1°C (for $V_{heat} = 5$ deg/min). The error in the determination of the melting heat for $V_{heat} = 5$ deg/min was ±5%, while for the heat of crystallization it was ±10%.

We note that the error in the determination of the absolute values of heat capacity, C_P, differed for heating and cooling modes and depended on the temperature range. In the heating mode, at temperatures above 0°C, it was ±5%; in the region below 0°C it was ±7.5%. In the cooling mode, the error in the C_P value was ±10%. The errors in the determination of C_P increased significantly when the heating/cooling rates used were decreased. In this regard, the curves of the dependence of the heat capacity on the temperature for $V_{heat} = 1$ and 2 deg/min were obtained as a result of averaging three thermograms recorded directly after each other. This procedure was quite justified, since the error in reproducing the experimental results using DSC-111 on a single sample at a fixed humidity was several times less than the standard error for different samples of the same humidity. In addition, the reproducibility of the results obtained at different times (sometimes with an interval of 1 or 2 years) was also very high.

Sephadex G-25 of the Pharmacia Fine Chemicals Company (Sweden) was chosen as the test subject. The data on the thermal properties of the freezing water in G-25 obtained in this work were compared with similar results for G-100 [39]. It is known that individual chains of polysaccharides in Sephadex are crosslinked by glycerol cross-bridges. G-25 differs from G-100 in a greater degree of their cross-linking [47]. The different degree of cross-linking of Sephadex also determines the difference in the ability to swell in the water medium due to a change in the spatial structure. Aqueous gels based on Sephadex are used in biochemistry as molecular sieves for the separation of biopolymers by molecular mass [48]. The volume of ultimate swelling of Sephadex in relation to the dry mass becomes greater as the cross-links in it become fewer. Each Sephadex globule is a polymer matrix, in which water clusters are embedded, whose size increases with increasing humidity of the system. It is important that this system is completely permeable to water molecules.

To study the thermal properties of small water clusters, only the initial degrees of swelling of $C_{H_2O} \leq 55\%$ were used. The total water content, including freezing and unfreezing water, in the studied G-25 varied from 10 to 55%. The required concentration of water in the samples in various experiments was set both by keeping them in a humid air environment (up to ≈40%) and by drying the swollen water gel at T_{room}. Preliminarily, the initial humidity of the preparation was determined by drying control samples in a vacuum at $T = 105$°C up to a constant mass, which for G-25 was of 9.6%. When the Sephadex samples with different degrees of hydration were prepared, the mass of the initial dry samples in all cases was almost the same (~30 mg), which made it possible to assume that the level of initial impurities in Sephadex, which were difficult to eliminate, remained unchanged during the humidification process. To establish a uniform humidity, the samples were placed in sealed steel ampoules and kept for 1 day at room temperature.

RESULTS AND DISCUSSION

The dependences of the temperature and heat of the melting and crystallization of the water clusters of different sizes included in the structure of Sephadex G-25 on humidity, as well as the relationship between their relative changes, were obtained in this study. All the regularities were established on the basis of the analysis of the recorded DSC thermograms of cooling/heating of the samples with different humidity (10–55% of water) in a wide range of temperatures (from –60 to ±25°C). Special attention was also paid to the processes that occurred when the samples were heated in the temperature range before melting in addition to melting and crystallization of water clusters directly. Experiments were also carried out to demonstrate the effect of the rate of scanning by temperature on the studied transitions, as well as stops during the DSC measurement. The new data obtained for water clusters in G-25 were compared with similar results for G-100 under similar humidity and measurement conditions.

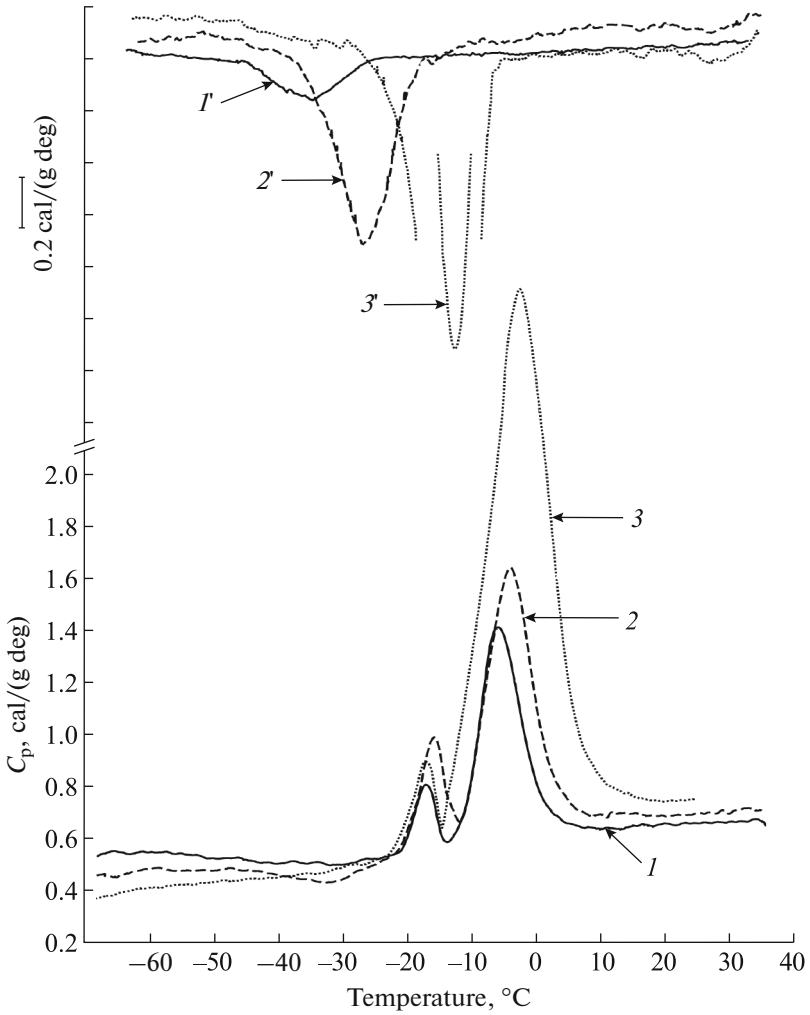

Fig. 1. The thermograms of cooling and heating in the crystallization region (*1'*, *2'*, *3'*) and melting (*1*, *2*, *3*) of the freezing water in Sephadex G-25 of different humidity: (*1*), 38.3% (solid line); (*2*), 44.5% (dashed line); and (*3*), 53.0% (dotted line); $V_{heat} = V_{cool} = 5$ deg/min.

It is believed that the observed melting curve of the frozen water reflects the distribution of water clusters by size [35–39]. However, since it was found in previous studies of starches and Sephadex G-100 that the initial water clusters can be reorganized during heating prior to the start of melting [38, 39], the question arose as to which distribution is fixed during thermal destruction in the transition interval: that one that was formed initially in crystallization during cooling or the one that was formed in the temperature range preceding melting during heating. The data obtained in this study enable us, in our opinion, to clarify this issue. The answer is also related to understanding the origin of hysteresis between the processes of melting and crystallization of water nanoclusters.

The Doublet Melting Curve of Water Clusters

The main peculiarity of the calorimetric data obtained for Sephadex G-25 was that the observed melting curves of the freezing water were bimodal for almost all the considered humidities (Fig. 1) in contrast to the corresponding single-modal curves for G-100. At the same time, the process of crystallization of the freezing water during cooling for the same humidity in both G-25 and G-100 was manifested in the form of single-modal curves (Fig. 1).

It was found that the two peaks of the melting curve clearly differed at the concentration of water in the sample in the range of 38–53%. At the same time, the intensity of the first, that is, the low-temperature peak, was significantly less than the high-temperature maximum in the entire humidity range.

The beginning of the melting curve of the frozen water characterizes the minimum size of clusters formed in the considered systems. At the same time, the temperature at the maximum of the curve corresponded to the melting of clusters of the most probable size. According to the data we obtained, in the case of

G-25, two sets of clusters with different most likely sizes were formed in the system. As mentioned, the Gibbs–Thomson formula can be used to estimate these sizes, since water clusters are located in the wet matrix of the polymer, that is, their absolute wetting is observed and $\cos\Theta = 1$ [35]. Our assessment of the size of water clusters in G-25 by their melting temperature has shown that we had two sets of the melting clusters with the most likely sizes of ~2 nm and ~5–15 nm depending on the humidity of Sephadex in the studied range.

The obtained doublet melting curves of the frozen water in the Sephadex G-25 indicated the appearance of an additional number of small water clusters compared to G-100. Their appearance could be associated with a large number of cross-links between polysaccharide chains and a corresponding reduction in the size of molecular sieves in G-25 compared to G-100. It was found that both the melting temperature and heat of the existing two sets of clusters changed differently with increasing humidity of G-25 to ~55%. While the thermal parameters of the melting of smaller water clusters (the first maximum) with increasing the Sephadex humidity remained virtually unchanged, within the error, the heat and temperature of the second maximum changed significantly.

We will discuss the obtained dependences of the main parameters of melting and crystallization of water nanoclusters on the humidity of Sephadex G-25 below in more detail.

The Temperatures of Melting and Crystallization of the Water Clusters

Figure 2 shows the temperatures of melting and crystallization of water clusters, as well as glass transition temperatures of the polymer matrix itself at different water content in G-25 in the range of 25–55%. It is important to note that in the humidity range of samples in which there was a doublet structure of the melting curve the graph shows T_{mel} for only the main high-temperature maximum. The previously obtained similar results for G-100 are also placed in the same figure for comparison.

It follows from the data we obtained (Fig. 2, curve *1*) that T_{mel} of water clusters decreased with a decrease in humidity of G-25, which was a typical manifestation of the size effect for nanosystems. At the same time, T_{cr}, which is less than T_{mel} for the entire studied humidity range, decreased even faster (Fig. 2, curve *2*); that is, the gap between the values of melting and crystallization temperatures, hysteresis, increased with decreasing cluster size. This phenomenon is also considered to be an important property of small systems. It is worth noting that the crystallization of the freezing water cooled to –60°C was not observed if the humidity of Sephadex was below 35%, which is due to the proximity to the glass transition region of the polymer. At the same time, the melting curves of the frozen water were presented on the thermograms during the subsequent heating. The obtained dependence of the glass transition temperature T_{gl} on the G-25 humidity (Fig. 2, curve *3*) showed how close the glass transition regions of the polymer and the possible crystallization of the freezing water were at these water concentrations. This means that the process of crystallization of water clusters in this temperature range was limited by the molecular mobility of the polymer matrix itself.

One can see that the dependences of T_{mel}, T_{cr}, and T_{gl} of water clusters on the polymer humidity obtained for G-25 practically coincided with the corresponding results for the previously studied Sephadex G-100 [39].

The Heats of Crystallization and Melting of the Water Clusters

Figures 3 and 4 demonstrate the obtained dependences of the heats of melting Q_{mel} and crystallization Q_{cr} of the freezing water in G-25 on humidity. The heat values shown in these figures reflect the results of processing the same data after different normalization. Figure 3 shows the heat of the studied processes after the normalization directly to the mass of the freezing water, which made it possible to obtain the actual values of Q_{mel} and Q_{cr} of water nanoclusters at different humidity of Sephadex. For this purpose, the boundary concentration between the freezing and non-freezing water in G-25 was preliminarily determined, below which the endothermic maximum related to the melting of the frozen water disappears from the heating thermograms. This concentration was 25%. The determination of the boundary between the frozen and unfrozen water was performed at the heating rate of 5 deg/min, which was used mainly in this work. Figure 4 shows the data on the heat of the studied transitions as the result of normalization to the mass of the entire sample for easy comparison with previously obtained similar results for G-100 and starches [37, 39].

We also note that in both processing methods, the total heats of the corresponding two maxima were used to calculate Q_{mel} of water clusters in the case of a bimodal melting curve.

As follows from the data shown in Fig. 3, Q_{mel} and Q_{cr} of water clusters in G-25 with humidity below 55% were significantly less than those of bulk water. At the same time, the heat of both transitions decreased with a decrease in the water content in this Sephadex (Figs. 3 and 4). The observed decrease in Q_{mel} of water clusters, as well as their T_{mel}, was associated with a typical manifestation of the size effect characteristic of nanosystems [25, 26, 36, 39–41]. This effect was obvious in the case of the normalization to the mass of freezing water (Fig. 3); while in the case of the normalization of the data to the total mass of the sample

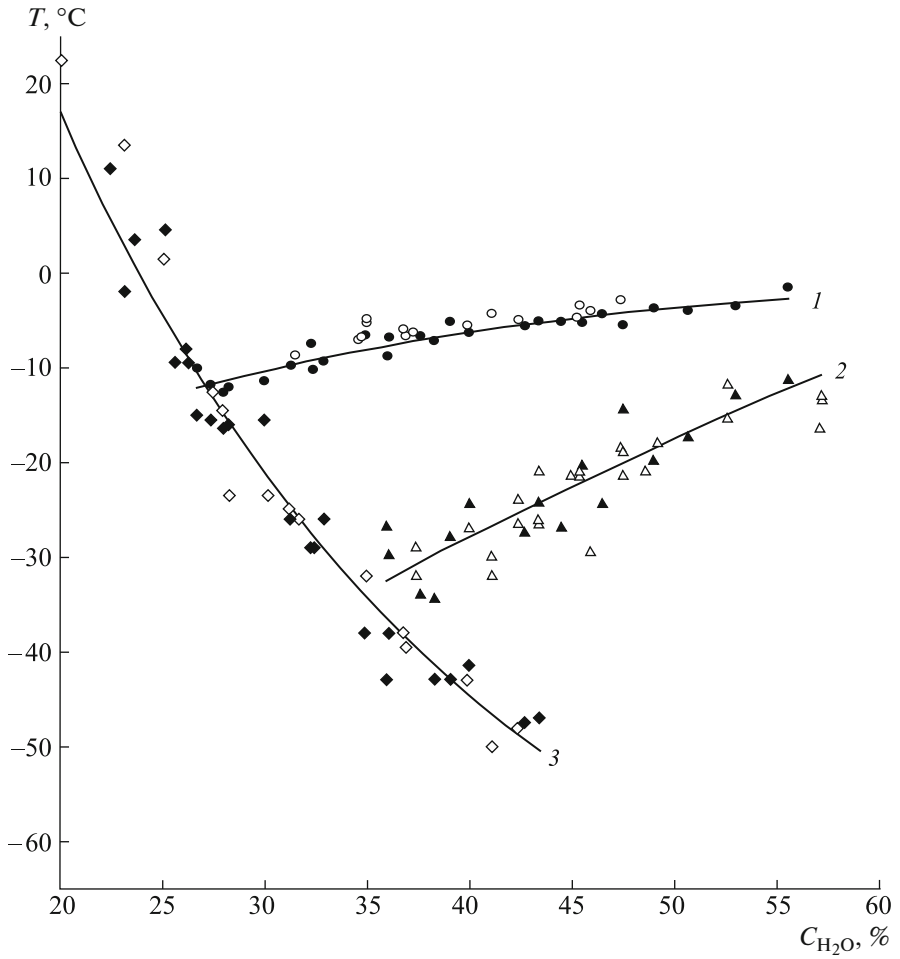

Fig. 2. The dependence of the temperature of melting (*1*) and crystallization (*2*) of water clusters, as well as the glass transition temperature of the polymer (*3*) on the humidity of Sephadexes G-25 (filled symbols) and G-100 (empty symbols) [39].

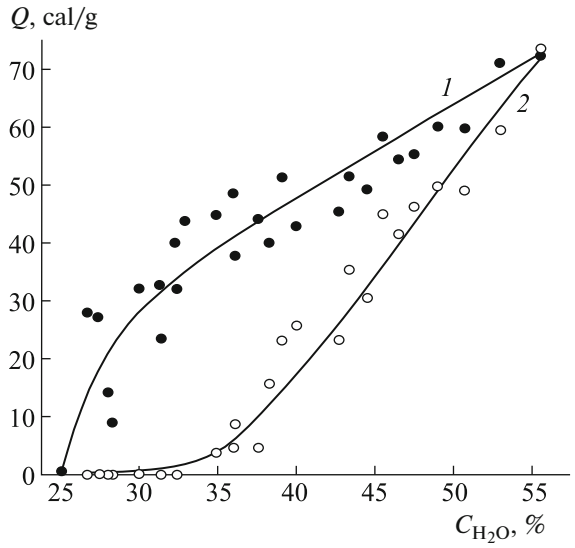

Fig. 3. The dependence of the heat of melting (*1*) and crystallization (*2*) of water clusters in Sephadex G-25 on its humidity. The given values of heat are normalized to the mass of the freezing water; $V_{heat} = V_{cool} = 5$ deg/min.

(Fig. 4), the existence of the size effect in the Q_{mel} of water clusters can be revealed only if one imagines the existing nonlinear dependence of the Q_{mel} (C_{H_2O}) as two straight lines, in the first approximation, with different angles of inclination, extrapolated to 100% water (for example, as in [49]).

The decrease in Q_{cr} with a decrease in water concentration was clearly manifested in any method of normalization (Figs. 3 and 4). It should be kept in mind that in G-25 with C_{H_2O} below ~35% at the conditions of the experiment, the process of crystallization of the freezing water was not observed at all ($Q_{cr} = 0$). Thus, the lower the humidity of G-25 was, the lower Q_{cr} and Q_{mel} were and, consequently, the size of the water clusters formed in the system.

We emphasize that there is practically no information about the dependence of the heat of crystallization on the size of nanoparticles in the literature. This is also true for direct measurement of the heat of melting and crystallization of nanoclusters in one experiment. The fact that these data were obtained using the

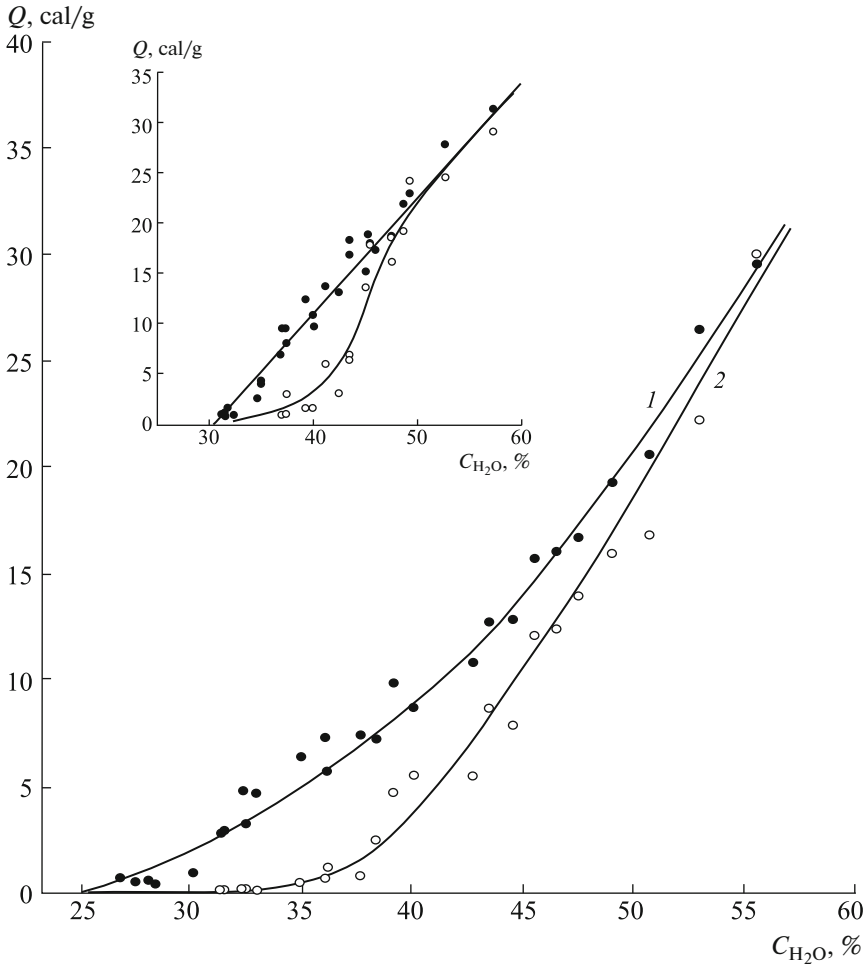

Fig. 4. The dependence of the heat of melting (*1*) and crystallization (*2*) of water clusters in Sephadex G-25 on the total water content in the sample. The given values of heat are normalized to the mass of the sample. The inset: similar dependencies for Sephadex G-100 [39].

DSC method in this study and in [37–39] is largely due to the choice of the object of study, namely, water nanoclusters, in which the processes of melting and crystallization occur in a convenient temperature range that is accessible to experimenters.

Comparison of the obtained dependences of the heats of melting Q_{mel} and crystallization Q_{cr} of water clusters on humidity in G-25 and G-100 [39], in addition to T_{mel} and T_{cr}, indicated that the thermal properties of water clusters in both types of Sephadex differed slightly at relatively low degrees of swelling, despite the difference in the spatial structures of their constituent globules, each of which can be considered as one giant macromolecule.

A Classic Manifestation of Hysteresis

The data shown in Figs. 3 and 4 also indicate that Q_{cr} of the freezing water decreased faster than Q_{mel}, and the difference between the values of the melting and crystallization heats, that is, hysteresis, increased with decreasing cluster size.

Thus, it has been shown above that hysteresis occurred between the melting and crystallization temperatures of water nanoclusters for both types of Sephadex, as well as for other polysaccharides (starches) [37, 38], $\Delta T = T_{mel} - T_{cr}$, and between the heats of these transitions, $\Delta Q = Q_{mel} - Q_{cr}$. At the same time, $T_{mel} > T_{cr}$ and $Q_{mel} > Q_{cr}$ in the studied humidity range. The most pronounced hysteresis between the parameters of the studied processes was manifested at the Sephadex humidity in the range of 35–40%. At a humidity of ~55%, according to the obtained data, the observed hysteresis for $\Delta T = T_{mel} - T_{cr}$ significantly decreased (Fig. 2); while hysteresis for $\Delta Q = Q_{mel} - Q_{cr}$ became almost invisible (see Figs. 3 and 4). With a further increase in the Sephadex humidity to greater than 55%, the melting and crystallization parameters of the freezing water tended to the corresponding values for the bulk water. The comparison of data concerning the

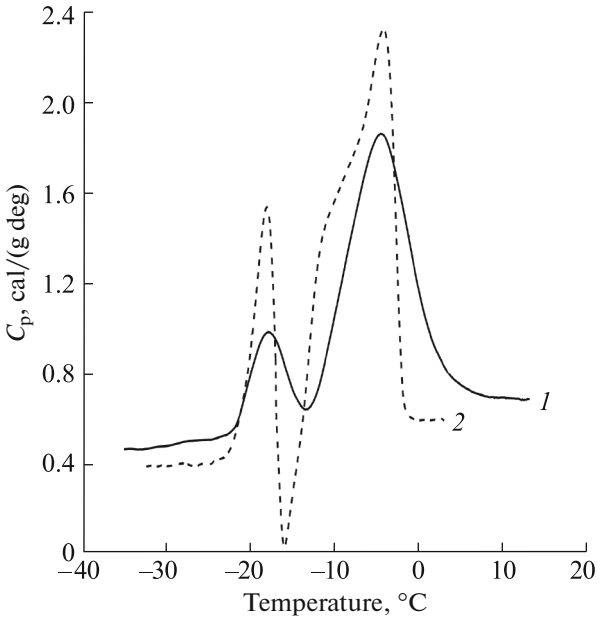

Fig. 5. The curve of melting of water clusters in Sephadex G-25 at different heating rates: (*1*) 5 deg/min; (*2*) 1 deg/min. $C_{H_2O} = 43.4\%$.

manifestation of hysteresis in the thermal properties of water nanoclusters in G-25 and G-100 [39] also showed their closeness to each other.

The Processes of Transformation of Water Nanoclusters in Polysaccharides

However, a difference was found in the thermal behavior of the two compared systems. It was manifested in the character of additional crystallization of supercooled water clusters along with the doublet structure of the melting curves of the frozen water obtained for G-25 during heating. As shown earlier, the additional crystallization of water clusters in G-100 during heating was identified by a clear minimum; the heat of this process was quite comparable to the heat of initial crystallization during cooling (for 40% Q_{cr} = 4 cal/g; $Q_{add.cr} \cong 4$ cal/g; and Q_{mel} = 12 cal/g) [39]. In other words, it was found that a new crystalline phase of water was added to the ice clusters that were formed during cooling after subsequent heating.

The thermograms of heating of G-25 also showed minima that reflected the transformation of initially formed water crystallites (for example, curve *2* in Fig. 1). However, the heat associated with this process in G-25 was much less than in Sephadex G-100; that is, this process was less intense in G-25. As an example, Q_{cr}, $Q_{add.cr}$, and Q_{mel} in G-25 at comparable humidity values were 4 cal/g, ~1 cal/g, and 10 cal/g, respectively (the experimental values were normalized to the mass of the sample). As well, there was another, much more expressed, manifestation of the transformation of the initial water crystallites in Sephadex G-25, as shown by the following experiments.

Figure 5 demonstrates the influence of the heating rate on the studied processes in the wet Sephadex G-25 (the relevant temperature corrections were taken into account). The results of averaging of the three-time sample heating at a rate of 1 deg/min are presented, as noted above. It can be seen that a decrease in the heating rate from 5 to 1 deg/min led to a significant change in the shape of the doublet curve of the melting of water clusters in G-25; namely, it led to a better resolution of the maxima of the observed doublet and to a deepening of the minimum between them, which, in turn, indicated the release of heat within the melting interval. In addition, a shoulder appeared at the second maximum at the low-temperature side of it. There was an increase in the area of the second maximum due to these changes. As a result, the total melting heat of water clusters Q_{mel} increased when the heating rate decreased (by ~3 cal/g against the background of ~12–13 cal/g at $C_{H_2O} = 43.4\%$).

The observed processes can be explained as follows. At the beginning of the melting interval, the smallest water crystals melted near –23°C (Fig. 1). Their size, determined on the basis of the Gibbs–Thomson equation, was 1–2 nm. After this, water nanoclusters crystallized again in the resulting melt, joined to larger clusters, and thereby increased their number, which was reflected in the appearance of a shoulder at the second maximum on the low-temperature side of the bimodal melting curve (Fig. 5). Since the Q_{mel} of water nanoclusters depended significantly on their size (Fig. 3), the resulting Q_{mel} increased.

Thus, the experiment has shown that the detected increase in Q_{mel} with a decrease in V_{heat} can be explained within the existing dependence of Q_{mel} on the size of the cluster, that is, by the size effect. The same explanation is applicable, in our opinion, for understanding the origin of hysteresis between the parameters of melting and crystallization of water clusters in general.

This conclusion can be further supported by another experiment conducted in this study, which demonstrated the influence of different modes of heat treatment of the samples on the obtained Q_{mel} of nanoclusters, in particular, stopping the scanning and annealing in the melting interval (Fig. 6). Curves *1* and *2* in Fig. 6 refer to the standard cycle of cooling–heating of the sample, in which, it should be emphasized, all processes were completely reproducible if the modes of temperature change were reproduced. The shape of the melting curve obtained after heating from –60°C of the crystallized sample, which was obtained by cooling at a temperature close to the minimum of the doublet, changed as a result of thermostating (annealing) for 30 min (curve *3*). The previously

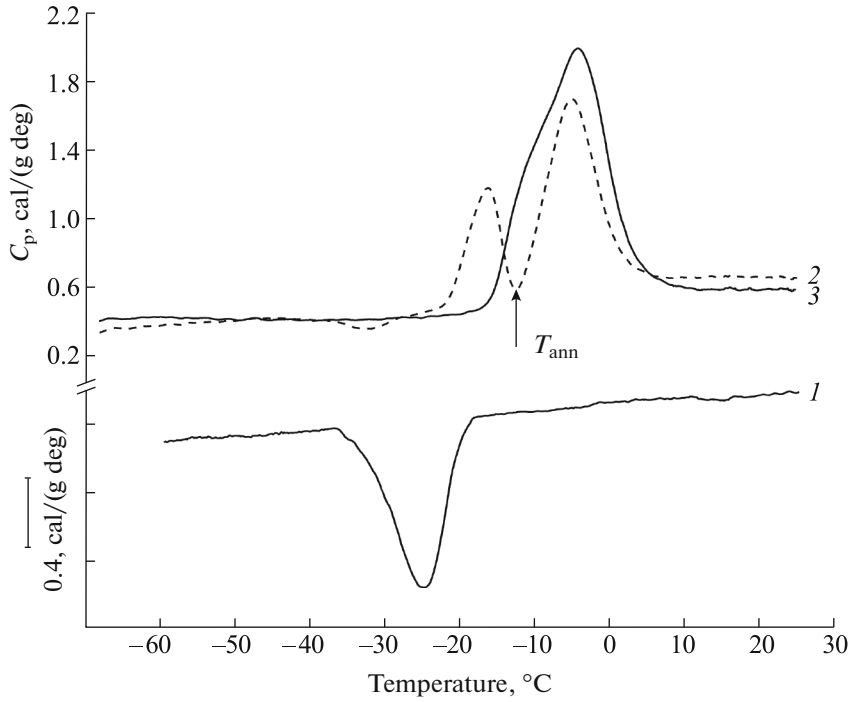

Fig. 6. The effect of annealing on the structure of the doublet in the melting curve of water nanoclusters in Sephadex G-25. C_{H_2O} = 44.5%; (*1*) and (*2*), cooling and subsequent heating (standard cycle); (*3*), heating the sample after annealing at $T = -12$°C. $t = 30$ min. $V_{heat} = V_{cool} = 5$ deg/min

observed first maximum of the doublet curve disappeared. It can be seen that in this case a shoulder appeared on the melting curve at the side of low temperatures caused by annealing, as in the previous experiment with a low heating rate, which indicated an increase in the initial distribution of the number of enlarged clusters of water. The melting heat Q_{mel} of water nanoclusters after such thermal treatment also increased (by ~4.5 cal/g against the background of ~14 cal/g at $C_{H_2O} = 44.5\%$). Thus, the initial distribution in the size of the clusters continued to change significantly in Sephadex G-25 as a result of the annealing. The small water crystallites disappeared during heating; the water clusters joined the larger ones during annealing causing the resulting Q_{mel} to increase.

The observed changes indicated that the system of supercooled water clusters in Sephadex was in nonequilibrium state; it was transformed when heated in the temperature range below 0°C both before the melting interval and inside it. All these processes contributed to the expression of hysteresis between the melting and crystallization parameters. At the same time, it is important to emphasize that the discussed transformation (reorganization and size change) of water clusters in polysaccharides occurred at the nanoscale. In this case, after the completion of the initial melting, repeated crystallization and melting of water crystallites demonstrated the reproduction of thermograms of the standard cycle ($V_{heat} = V_{cool}$) and complete erasure of the memory on the previous thermal testing. This reorganization at the nanoscale significantly differs from the irreversible transformation of clusters in starch-containing products at the microscale, which was studied by optical methods [50].

CONCLUSIONS

The previous cycle of studies on the thermal properties of water clusters in polysaccharide–water systems (starch and Sephadex G-100) with a low content of freezing water was continued in this work. This DSC study based on the example of another modified polysaccharide with a different spatial structure, namely, Sephadex G-25, made it possible not only to detect a number of distinctive features of the processes of crystallization and melting of frozen water in G-25, but also to generalize the obtained data on the thermal behavior of water clusters in wet polysaccharides.

The main peculiarity of the calorimetric data obtained for Sephadex G-25 is that the observed melting curves of water clusters had a doublet structure for almost all humidity values considered in the work (except the lowest value), in contrast to the corresponding single-modal curves for G-100. This reflected the bimodal distribution of clusters by size; that is, the possibility of formation of two sets of

water clusters with different most likely sizes (~2 nm and 5–15 nm depending on the hydration of Sephadex) in G-25 with its more rigid spatial organization compared to G-100. At the same time, the process of crystallization of the freezing water during cooling for the same humidity values in both G-25 and G-100 was manifested in the form of single-modal curves.

Moreover, the difference in the spatial structures of G-25 and G-100 practically did not affect the manifestation of the size effect, which is characteristic of small systems, in the obtained dependencies of the temperatures and heat of melting and crystallization of water nanoclusters on the humidity of Sephadex. In addition, hysteresis was revealed for water nanoclusters in both Sephadexes, as well as in starch, between their melting and crystallization temperatures for these transitions, $\Delta T = T_{mel} - T_{cr}$ and between the heats $\Delta Q = Q_{mel} - Q_{cr}$, which also demonstrated their similarity with regard to the character of changes that depend on humidity.

It was also common for all the studied polysaccharides with low humidity that the transformation processes in the system of clusters of crystallized supercooled water occurred during both heating below the melting interval and inside it. In the region before melting, the reorganization might be manifested either as a slight decrease in the absolute values of the heat capacity, as in the amorphization of native starch, or, as in the case of G-25 and G-100, as an additional clearly expressed exothermic maximum on the thermograms of heating. In other words, it was due to the appearance of a new crystalline phase of water during heating in the region before melting. We note that in Sephadex with a low content of freezing water, the first stage of its crystallization during cooling occurred near the glass transition temperature, when the mobility of the macromolecular matrix itself decreased. This is the reason that crystallization of water clusters in G-25 was not detected at humidity below 35%. With increasing humidity of Sephadex and, accordingly, greater distance from the glass transition temperature, the increased mobility of polysaccharide chains provided sufficient mobility for both crystallization during cooling and for additional crystallization during heating of small water clusters that moved freely between individual cells of the molecular sieve.

The processes of reorganization of water clusters that initially crystallized during cooling were most clearly manifested in Sephadex G-25 in the interval of their melting. Their manifestation depended on the heating conditions. First, when V_{heat} decreased, there was a change in the intensities of the components of the doublet in the melting curve. Second, small clusters were enlarged during annealing within the melting interval; and, accordingly, the heat of melting increased due to the revealed size effect. It should be noted that it was probably possible to detect these changes because the rates of the considered processes of transformation of clusters were comparable with the heating rates used in the work.

All these processes, together and separately, indicated the nonequilibrium state of the initial set of water nanoclusters that crystallized during cooling in Sephadex. Recall that a similar nature of the process of reorganization of nanocrystallites, as observed in synthetic polymers, was also considered as a consequence of the nonequilibrium state of the initial crystallites formed under significant supercooling relative to the melting temperature.

Thus, the nonequilibrium state of supercooled water clusters in all polysaccharide–water systems that we studied, and, as a consequence, their ability to transform with increasing temperature up to melting is, in our opinion, one of the possible causes, if not the main cause of the hysteresis phenomena discussed above. The results obtained in this study demonstrated that the transformation leading to an increase in the size of the initially formed during cooling crystallites and, accordingly, to the observed increase in the temperatures and heats of their melting, is certainly an important factor in the hysteresis manifestation in the thermal properties of water nanoclusters.

In conclusion it should be emphasized that the results of the conducted research provided an unambiguous answer to the question posed at the beginning of the study about which distribution of the crystallized water clusters in Sephadex melts in the transition interval. It was reliably determined that the observed melting curve reflected the thermal destruction of a new set of water nanoclusters that arose as a result of various kinds of restructuring processes (additional crystallization, reorganization, and size changes) rather the original set.

COMPLIANCE WITH ETHICAL STANDARDS

The authors declare no conflict of interest. This paper does not describe any research using humans and animals as objects.

REFERENCES

1. G. N. Makarov, Usp. Fiz. Nauk **180**, 185 (2010).
2. P. Pawlow, Z. Phys. Chem. **65**, 545 (1909).
3. I. V. Sochava, G. I. Tsereteli, and O. I. Smirnova, Fiz. Tverd. Tela **14** (2), 553 (1972).
4. B. Wunderlich, *Macromolecular Physics* (Academic, New York, 1980; Mir, Moscow, 1984), Vol. 3.
5. Yu. K. Godovsky, *Thermophysical Methods of Polymer Research* (Khimiya, Moscow, 1976) [in Russian].
6. V. A. Bershtein and V. M. Egorov, *Differential Scanning Calorimetry in Physicochemistry of Polymers* (Khimiya, Leningrad, 1990) [in Russian].
7. I. V. Sochava and G. I. Tsereteli, Vysokomol. Soed. **13** (2) 155 (1971).
8. G. I. Tsereteli and I. V. Sochava, Vysokomol. Soed. **13** (11) 2612 (1971).

9. H. Haberland, T. Hippler, J. Donges, et al., Phys. Rev. Lett. **94**, 035701 (2005).
10. M. Schmidt, R. Kusche, B. von Issendorff, et al., Nature **393**, 238 (1998).
11. M. Schmidt, R. Kusche, T. Hippler, et al., Phys. Rev. Lett. **86**, 1191 (2001).
12. R. Berry, in *Clusters of Atoms and Molecules: Theory, Experiment, and Clusters of Atoms* (Springer, Berlin, 1994), Ch. 2.8.
13. G. A. Breaux, C. M. Neal, B. Cao, and M. F. Jarrold, Phys. Rev. Lett. **94**, 173401 (2005).
14. R. S. Berry and B. M. Smirnov, Usp. Fiz. Nauk **175**, 367 (2005).
15. R. S. Berry and B. M. Smirnov, Usp. Fiz. Nauk **179**, 147 (2009).
16. D. J. Wales and R. S. Berry, Phys. Rev. Lett. **73**, 2875 (1994).
17. R. S. Berry, Nature **393**, 212 (1998).
18. D. J. Wales, Adv. Chem. Phys. **115**, 1 (2000).
19. R. S. Berry and B. M. Smirnov, Zh. Eksp. Teor. Fiz. **127**, 1282 (2005).
20. F. Caupin, Phys. Rev. B **77**, 184108 (2008).
21. C. Alba-Simionesco, B. Coasne, et al., J. Phys.: Cond. Matter **18**, R15 (2006).
22. B. F. Borisov, E. V. Charnaya, P. G. Plotnikov, et al., Phys. Rev. B, **58** (9), 5329 (1998).
23. G. Kellermann and A. F. Craevich, Phys. Rev. B **65**, 134204 (2002).
24. S. L. Lai, et al., Phys. Rev. Lett. **77**, 99 (1996)
25. H. M. Lu, F. Q. Han, and X. K. Mong, J. Phys. Chem. B **112**, 9444 (2008).
26. A. Moitra, et al., J. Phys. D **41**, 185406 (2008).
27. *Water Relationships in Foods,* Ed. by H. Levine and L. Slade (Plenum, New York, 1991).
28. G. M. Mrevlishvili, *Low-Temperature Calorimetry of Biological Macromolecules* (Metsniereba, Tbilisi, 1984) [in Russian].
29. G. I. Tsereteli, T. V. Belopolskaya, and T. N. Melnik, Biofizika **42** (1), 68 (1997).
30. T. V. Belopolskaya, G. I. Tsereteli, N. A. Grunina, et al., in *Starch: Recent Advances in Biopolymer Science and Technology,* Ed. by M. Fiedorowicz and E. Bertoft (Polish Society of Food Technologists, Malopolska Branch, 2010), pp. 29–44.
31. T. V. Belopolskaya, G. I. Tsereteli, N. A. Grunina, et al., in *Starch Science Progress,* Ed. by L. A.Wasserman, G. E. Zaikov, P. Tomasik, (Nova Science Publ., New York, 2011), pp. 1–15.
32. K. Tananuwong and D. S. Reid, Carbohydrate Polym. **58**, 345 (2004).
33. S. Suzuki and S. Kitamura, Food Hydrocolloids **22**, 862 (2008).
34. T. Tran, K. Thitipraphunkul, K. Piyachomkwan, et al., Starch/Stark **60**, 61 (2008).
35. S. Park, R. A. Venditti, H. Jameel, et al., Carbohydrate Polym. **66**, 97 (2006).
36. N. A. Grunina, G. I. Tsereteli, T. V. Belopolskaya, and O. I. Smirnova, Carbohydrate Polym. **132**, 499 (2015).
37. G. I. Tsereteli, T. V. Belopolskaya, N. A. Grunina, et al., Biophysics (Moscow) **62** (1) 43 (2017).
38. T. V. Belopolskaya, G. I. Tsereteli, N. A. Grunina and O. I. Smirnova, Biophysics (Moscow) **62** (5) 696 (2017).
39. G. I. Tseretely, T. V. Belopolskaya, N. A. Grunina and O. I. Smirnova, Biophysics (Moscow) **64** (1) 14 (2019).
40. W. Hu, S. Xiao, J. Yang, and Z. Zhang, Eur. Phys. J. B **45**, 547 (2005)
41. M. Binnewies and E. Milke, *Thermochemical Data of Elements and Compounds* (Wiley-VCH, Weinheim, 1999).
42. T. L. Beck, J. Jellinek, and R. S. Berry, J. Chem. Phys. **87**, 545 (1987).
43. H. L. Davis, J. Jellineh, and R. S. Berry, J. Chem. Phys. **86**, 6456 (1987).
44. B. M. Smirnov, Usp. Fiz. Nauk **177**, 369 (2007).
45. A. M. Malvezzi, M. Allione, M. Patrini, et al., Phys. Rev. Lett. **89**, 087401 (2002).
46. T. Bachels, H.-J. Guntherodt, and R. Schafer, Phys. Rev. Lett. **85**, 1250 (2000).
47. T. Devenyi and J. Gergely, *Amino Acids, Peptides and Proteins: Biochemical and Immunochemical Techniques in Protein Chemistry* (Elsevier Science, 1974; Mir, Moscow, 1976).
48. T. G. Plachenov and S. D. Kolosentsev, *Porosity Measurement* (Khimiya, Leningrad, 1988) [in Russian].
49. N. A. Grunina, G. I. Tsereteli, T. V. Belopolskaya, et al., in *Starch Science and Technology*, Ed. by V. P. Yuriev, P. Tomasik, (Nova Science Publ., Inc. New York, 2008), pp. 77–87.
50. H. D. Goff, in *Starch in Food: Structure, Function and Application*, Ed. by A.-C. Eliasson (Woodhead Publ., Cambridge, 2004), pp. 425–427.

Translated by E. Puchkov